Biochemistry

 Volume 39, Number 34 August 29, 2000

Accelerated Publications

Hanging Gondola Structure of the T1 Domain in a Voltage-Gated K^+ Channel†

William R. Kobertz, Carole Williams, and Christopher Miller*

Department of Biochemistry, Howard Hughes Medical Institute, Brandeis University, Waltham, Massachusetts 02454

Received June 6, 2000; Revised Manuscript Received July 3, 2000

ABSTRACT: The T1 domain is a ~100-residue sequence in the cytoplasmic N-terminal region of K_v-type K^+ channels. The structure of the isolated domain is known, but it is uncertain whether the structure of this domain is maintained in the fully assembled, membrane-associated, homotetrameric channel protein. We use the structure of the isolated domain as a guide for designing disulfide bonds to cross-link Shaker K^+ channels through the T1 domain. Six pairs of residues with side chains closely apposed across the T1 subunit interface were selected for replacement by cysteine. Of these, three pairs formed cross-links upon air oxidation of cysteine-substituted Shaker channels expressed in Xenopus oocyte membranes. Two of these cross-linked channels were examined electrophysiologically and were found to have gating properties only slightly altered from wild-type. The results show that the structure of the isolated T1 domain exists in the mature ion channel. They also demand that this domain is attached to the membrane-embedded part of the protein as a cytoplasmic "hanging gondola", and that ions gain access to the pore through four "windows" formed by the linker connecting T1 to the channel's first transmembrane helix.

Cellular electrical signals are fashioned by the coordinated action of ion channel proteins, among which the voltage-gated K^+ channels are the most intensely studied from a structural viewpoint (*1*, *2*). These K_v-type channels are tetrameric integral membrane proteins constructed according to a barrel-stave plan in which four identical or similar polypeptide subunits surround the K^+ permeation pathway formed on the symmetry axis. The membrane-embedded part of the generic K_v subunit, made up of ~250 residues spanning six transmembrane helices S1−S6, is composed of two parts: the pore-forming domain, S5−S6, and the voltage-gating domain, S1−S4 (Figure 1A). In the Shaker channel, typical of the K_v family, only ~30% of the protein resides within the membrane, and this is flanked by two cytoplasmic segments making up the preponderance of the channel's mass: the ~220-residue N-terminus and the ~150-residue C-terminus.

Over the past decade, structure−function studies of K_v channels have focused mainly on the membrane-associated part of the protein, where ion-selective permeation and voltage-dependent gating occur (*2*). Only recently has the cytoplasmic region of these channels come under scrutiny, in the wake of the high-resolution structure determination of the isolated T1 domain (*3*, *4*), a ~100 residue conserved sequence preceding the first transmembrane helix. The T1 domain is known to carry out two separate functions in K_v channels. It is responsible for subunit segregation, i.e., for preventing K_v subunits of different molecular subfamilies from co-assembling within the same tetramer (*5*, *6*); in addition, it presents a docking platform for the K_v β-subunits that regulate some, but probably not all, voltage-gated K^+ channels (*7*, *8*). When expressed alone, the isolated T1 domain forms a water-soluble homotetramer with 4-fold symmetry (*3*, *9*), a characteristic unusual for a globular

† Supported in part by NIH grant GM-31768.

* To whom correspondence should be addressed. E-mail: cmiller@brandeis.edu. Phone: (781) 736-2340. Fax: (781) 736-2365.

10.1021/bi001292j CCC: $19.00
Published on Web 08/03/2000

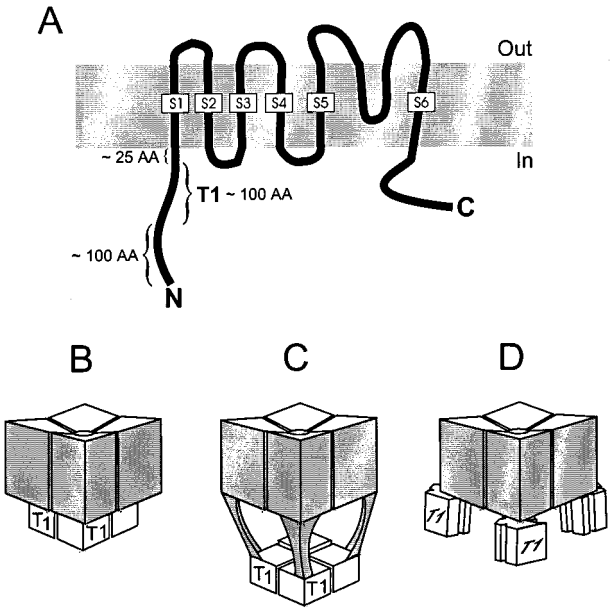

FIGURE 1: Models for T1 attachment to K_v channels. (A) Transmembrane topology model of the K_v channel family. (B) Cytoplasmic pore model, in which the T1 domain is continuous with the permeation pathway. (C) Hanging gondola model, in which the tetrameric T1 domain is separated from the permeation pathway. (D) Cytoplasmic vestibule model, in which the T1 domain adopts a structure in the fully assembled channel different from the tight tetramer of the isolated domain.

protein but natural in a tetrameric membrane protein.

The question we address here is one that has recently been the subject of some contention: does the structure determined for the isolated T1 domain apply in the context of the native channel? There are several ways to imagine the domain attached to the membrane-embedded parts of the channel, as outlined previously (*10*−*12*). One possibility (Figure 1B) is that T1 adopts the same tetrameric structure seen in isolation and is continuous with the cytoplasmic end of the transmembrane pore. A related possibility (Figure 1C) is that the T1 tetramer, while coaxial with the pore, is not welded to it but instead hangs from the membrane-associated parts of the protein, as a gondola below a dirigible; this hanging gondola formation demands that cytoplasmic pore-access must be through four "windows" formed by "cables" linking T1 to the S1 transmembrane helix. A final possibility—not inconsistent with any previously known facts—is that the structure of isolated T1 exists only during the early stages of protein translation and that this tetramer is pulled apart as the channel is inserted into the membrane and assembled into its final structure (Figure 1D). In an earlier report, we ruled out the first possibility by showing that permeation and inactivation characteristics of Shaker K^+ channels are essentially unaltered by complete deletion of the T1 sequence (*10*). We now show that the structure of the isolated T1 domain faithfully predicts cross-subunit pairs of residues at which cysteine substitutions lead to covalently cross-linked Shaker channels. This result requires that the channel accommodates T1 as a hanging gondola.

EXPERIMENTAL PROCEDURES

Materials. NBT (nitro blue tetrazolium), BCIP (5-bromo-4-chloro-3-indolyl phosphate), and the alkaline phosphatase-conjugated goat anti-mouse antibody used for Western blot analysis were from Promega. Monoclonal antibody 1D4 (*13*) was a gift from Dan Oprian and was purified according to standard protocols (*14*). PNGase F was from NEB.

Recombinant DNA Methods. The "wild-type" channel used in these experiments is a previously described (*10*) inactivation-removed (Δ6−46) Shaker B with two additional modifications. First, two natural cysteines capable of forming a cross-subunit disulfide bond (*15*) were replaced by inert residues (C96S/C505A); second, an 8-residue epitope was appended to the C-terminus (*16*) to permit detection in oocyte membranes by the 1D4 antibody (*13*). Cysteine point mutants were made on this background in pBluescript KS(−) using PCR-based mutagenesis between 5′ *Nco*I and 3′ *Xba*I sites. All constructs were confirmed by sequencing through the cloning cassette, and cRNA was transcribed with T7 polymerase from a FspI-linearized plasmid.

Oocyte Membrane Preparation. Ooctyes were injected with 27 nL of cRNA (3 mg/mL) and were incubated at 17 °C in ND96-gentamicin solution (*17*) for 2−3 days. Batches of 40−50 oocytes were homogenized under reducing conditions in 1 mL of buffer HEDP (100 mM Hepes-NaOH, pH 7.6, 1 mM EDTA, 5 mM DTT,[1] PMSF 100 μg/mL) and kept at 4 °C during all subsequent steps. Following centrifugation (3000*g*, 10 min) the supernatant was collected and the pellet vigorously resuspended in 1 mL of buffer HEDP. Centrifugation was repeated and the supernatants (∼2 mL) combined. The homogenate was overlaid on a 15% sucrose cushion prepared in 100 mM Hepes-NaOH, pH 7.6, and subjected to centrifugation (175000*g*, 75 min). The membrane pellet was resuspended in PBS (pH 7.6) supplemented with 100 mM KCl and sucrose and then stored at −80 °C. For *N*-ethylmaleimide (NEM) treated samples, 5 mM NEM was included in buffer HEDP and in the sucrose cushion, and DTT was omitted. Samples treated with H_2O_2 also contained 1 mM EGTA in the resuspension buffer and the sucrose cushion.

Disulfide Cross-Linking. Disulfilde cross-links readily formed (10−60 min) at room temperature with ambient oxygen. Rapid cross-linking was induced by treatment with 0.01−0.1% H_2O_2 for 2−5 min at room temperature. The reactions were terminated by the addition of gel loading buffer (*18*) containing 12 mM NEM. For reducing gels, NEM was omitted from and 5% (v/v) β-mercaptoethanol was included in the stop solutions. For deglycosylation after oxidation reactions, membrane samples (10 μL) were first treated with 1 mM NEM for 10 min. Excess NEM was then base-hydrolyzed by adding 3 μL of 0.5 M Tris-HCl (pH 8.6); 1.5 μL of 10% SDS was also added at this point, and the mixture was incubated for 4 h at 37 °C. After hydrolysis, NP-40 (3 μL, 10%), water (11 μL), and PNGase F (1 μL, 500 units/μL) were added, and after 1 h at 37 °C, reactions were stopped by addition of Laemmli load buffer.

Western Blot Analysis. Protein samples were separated by electrophoresis on 7.5% SDS−polyacrylamide gels using standard loading solutions (*18*). The proteins were transferred to nitrocellulose and blocked with 5% BSA, 150 mM NaCl, 10 mM Tris-HCl, pH 7.4, for 20 min at 37 °C. Primary incubation with 1D4 antibody (4 μg/20 mL of blocking buffer) overnight was followed by washing (4 × 5 min) in

[1] Abbreviations: NEM, *N*-ethylmaleimide; DTT, dithiothreitol.

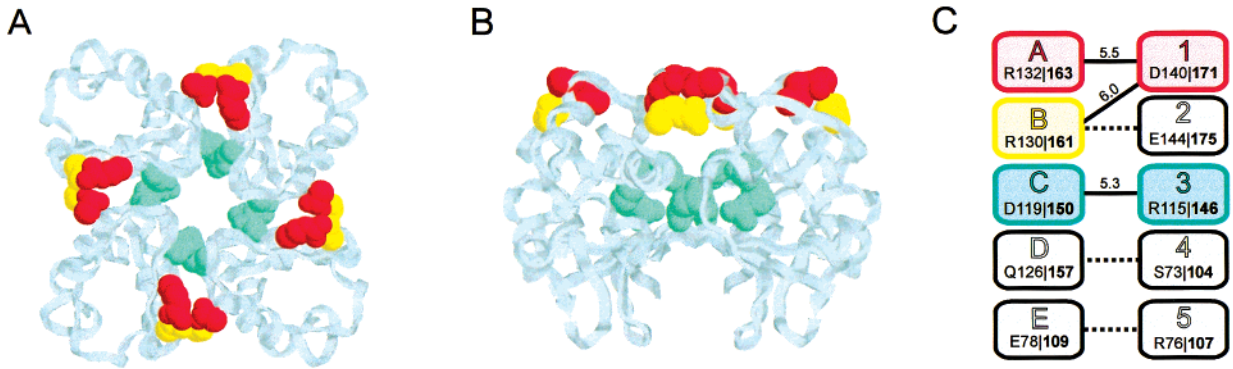

FIGURE 2: Interacting residues on the T1 subunit interface. Isolated T1 domain of *Aplysia* $K_v1.1$ is shown in two views. (A) Along the 4-fold axis from the C-terminal end; (B) perpendicular to the axis, with C-terminal end up. Space-filled side chains represent residues that form disulfide cross-links. (C) Schematic representation of interface residues chosen for cysteine substitution, with lines showing the pairwise contacts in the structure. Each position is labeled with a code (A−E, 1−5), the residue number and the equivalent position (in bold) in *Drosophila* Shaker. Since the T1 sequence is highly conserved (87% identity between *Drosophila* and *Aplysia* Shaker), there is no ambiguity in equivalence of residues. Colors on schematic match side chain colors on structure, and distances (in angstroms) between γ-carbons of these side chains are indicated on schematic. White residues and dashed lines on schematic identify pairs of cysteine substitutes that fail to form cross-links.

0.05% NP-40, 150 mM NaCl, 10 mM Tris-HCl, pH 7.4, and subsequent addition of alkaline phosphatase (AP)-conjugated goat anti-mouse (5 μL/20 mL, 30 min); blots were developed using NBT/BCIP reagents according to directions supplied by the manufacturer (Promega).

Electrophysiology. Standard techniques were used for preparation of and recording from *Xenopus* oocytes by excised macropatch methods (*17*). Ooctyes were injected with 50 nL of cRNA (0.5 mg/mL) and then incubated at 17 °C in ND96-gentamicin solution for 2−5 days. Inside-out patches were formed on 1−2 MΩ firepolished electrodes, and data were filtered at 2 kHz and sampled at 10 kHz. All solutions contained: 100 mM KCl, 1 mM EGTA, and 5 mM Hepes-KOH, pH 7.6. Pipet solutions also contained 1 mM $MgCl_2$. Reducing bath solutions contained 1 mM DTT and oxidizing bath solutions contained 0.01−0.1% H_2O_2. Standard voltage-activation experiments employed a holding potential of −90 mV and a family of 50-ms command pulses ranging from −80 to 40 mV in 5 mV increments followed by a 100 ms tail pulse to −80 mV. Some experiments used a pre-inactivation protocol, as follows. A macropatch was excised from the oocyte, and a voltage-activation family was collected as above. The patch was then depolarized to zero voltage for 10 min to produce >95% C-inactivation. With the patch maintained at zero voltage, H_2O_2 was applied for 2 min and then washed away. The patch was returned to −80 mV for 5 min to recover from C-inactivation, and another set of voltage-activation pulses was recorded.

Data Analysis. Tail-current amplitudes were measured 1−1.5 ms into the tail pulse. Voltage-activation curves were calculated using standard tail-current analysis (*19*). Data were fit to a Boltzmann function, $I/I_{max} = 1/\{1 + \exp[-zF(V - V_o)/RT]\}$, to determine V_o (half-maximal activation voltage) and z (slope factor).

RESULTS

The isolated T1 domain from a close Shaker orthologue, *Aplysia* $K_v1.1$, exists as a homotetramer in aqueous solution, from which it was crystallized for X-ray structure determination (*3*, *4*, *12*). But does the structure of the isolated domain (Figure 2, panels A and B) exist in the fully assembled protein? If this structure is preserved in the channel, then it should serve as a trustworthy template for designing disulfides that would cross-link Shaker subunits. Accordingly, we chose residues with side chains close enough in space to make cross-subunit salt bridges or H-bonds and replaced these in various combinations with cysteine. Ten residues participating in six pairwise side-chain interactions (Figure 2C) were selected, five on one side of the interface denoted A−E and five on the other side, denoted 1−5.

Our first goal was to screen these positions quickly for disulfide formation. To this end, subunits containing *single* cysteine replacements were coexpressed in pairs in *Xenopus* oocytes. All constructs produced robust K^+ currents with essentially normal characteristics. After 2−3 days of expression, oocyte membranes were prepared and exposed to mild oxidizing conditions (10−60 min in air-saturated buffer). The samples were run on SDS−PAGE gels and transferred to nitrocellulose for detection of Shaker protein. Immunoblots shown in Figure 3A demonstrate that three of the selected mixtures—C+3, B+1, and A+1—form dimeric Shaker protein upon air oxidation, while the wild-type channel remains fully monomeric. Glycosylation of Shaker protein (*20*) leads to a complex pattern of monomeric bands for wild-type and all cysteine mutants: a core-glycosylated band (~75 kDa) and a smeary doublet of fully processed material (~100 kDa). Disulfide formation between the subunit pairs above is revealed by the appearance of new bands running in the 150−180 kDa range. Simplification (*20*) of these banding patterns is readily accomplished by enzymatic deglycosylation of the samples (PNGase F lanes, Figure 3A). Following this treatment, monomer samples collapse to a single band of ~70 kDa, close to the size expected from the sequence (67 kDa), while cross-linked samples show one additional band (~150 kDa) corresponding to a dimer. In these mixtures of cysteine-substituted subunits, higher-order oligomers never appear upon oxidation, nor do the monomeric subunits disappear completely. To test the specificity of the cross-links, we examined interface residues that do not pair with each other in the crystal structure. Such mismatched residues fail to form cross-links upon oxidation: C+1, A+3, and B+3 (Figure 3A); other pairs of residues that do not cross-link

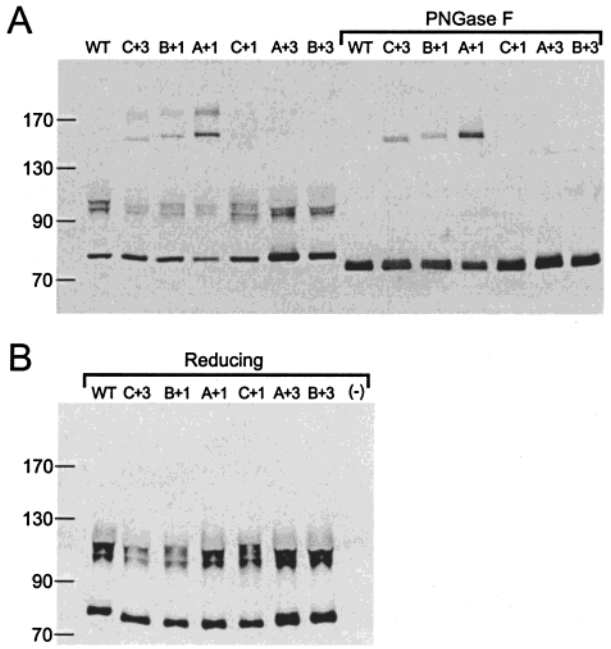

FIGURE 3: Cross-linking of mixed Shaker subunits at the T1 subunit interface. Immunoblots are from membrane preparations from Xenopus oocytes expressing the indicated Shaker constructs subjected to 10−60 min of air oxidation. Molecular weight standards are indicated on left. (A) Air oxidation only, before and after deglycosylation (PNGase lanes). (B) Air oxidation followed by reduction with 5% β-mercaptoethanol. Lane marked (−) represents uninjected control oocytes.

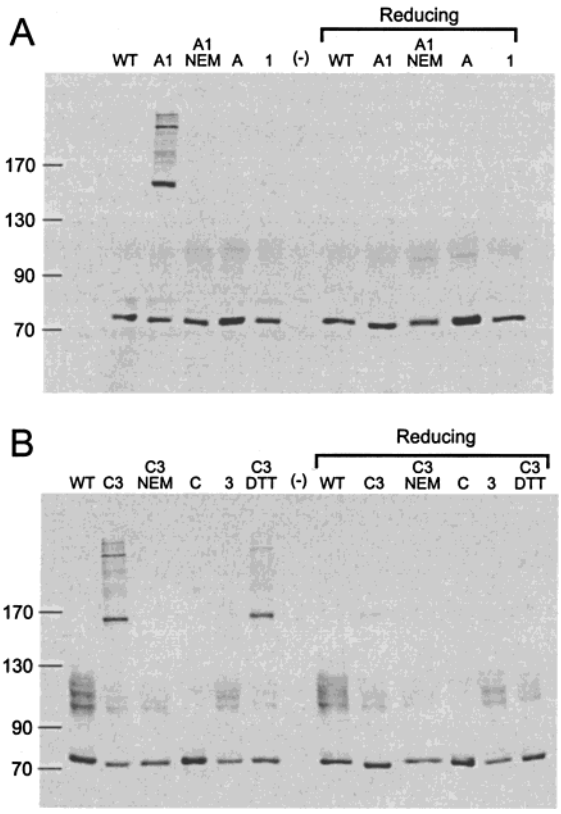

FIGURE 4: Cross-linking in a doubly substituted Shaker. Immunoblots as in Figure 3, with Shaker constructs containing double cysteine substitutions A1 (panel A) and C3 (panel B), along with the indicated single-cysteine or wild-type controls. Lanes marked "NEM" indicate samples pretreated with NEM before oxidation conditions; lanes marked "DTT" indicate samples treated with DTT (1 mM, 5 min) after air oxidation.

are B+2, D+4, E+5, A+4, D+1, C+2, and E+4 (data not shown). Samples pretreated with NEM (data not shown) before oxidation conditions, or treated with high concentration of β-mercaptoethanol (Figure 3B) after oxidation run strictly as monomers.

Since the channels used above are combinatorial mixtures of coexpressed single-cysteine replacements, we do not expect, nor do we observe, higher oligomers upon oxidation. But we do expect high-order cross-linking for homotetrameric channels carrying appropriate double-cysteine mutations. This expectation is confirmed with two separate pairs of disulfide-forming subunits: A1 (Figure 4A) and C3 (Figure 4B), which bear both mutations in the same subunit. Mild oxidation of these double mutants now produces higher oligomers, probably trimers and tetramers (*15*) along with dimers. These results are validated by several clean negative controls: wild-type, single cysteine replacements, NEM pretreatment, and disappearance of oligomers on reducing gels (Figure 4).

We investigated the functional consequences of cross-linking in inside-out macropatches containing double-mutant C3 channels (Figure 5). In such experiments, it is impossible to chemically assay the cross-linking status of the channels in the patch pipet. Accordingly, we applied oxidizing conditions (0.01−0.1% H_2O_2) strong enough to ensure that all subunits would be cross-linked within a few minutes. Under these conditions in oocyte membranes, C3 monomer bands are completely converted into higher oligomers, while wild-type and single-cysteine controls remain unaffected (Figure 5A). In inside-out macropatches expressing C3 channels, H_2O_2 increases the current at negative but not positive voltage (inset, Figure 5B). The enhancement of current, complete in ∼2 min (not shown), reflects a small (6 mV) leftward shift in the voltage-activation curve (Figure 5B), not observed with wild-type channels (Figure 5C). The shift of C3 gating is prevented but not reversed by 1 mM DTT (not shown), a failure that parallels the lack of DTT reversal of cross-linking seen in oocyte membranes under similar conditions (Figure 4B). Identical experiments performed with a second double-cysteine channel, A1, yielded similar results: a slight (11 mV) leftward shift in the activation curve. The effects of H_2O_2 on gating parameters for A1, C3, and wild-type channels are reported in Table 1.

Oxidation experiments on A1 channels were compared under two conditions. With standard recording conditions, oxidant was applied at a holding potential of −80 mV, i.e., with the channel closed. Alternatively, to mimic the depolarized voltage of the membrane fragments used for immunoblots, we employed a pre-inactivation protocol, holding the patch at zero voltage for 10 min and only then applying H_2O_2; in this way, the channels were in the C-inactivated conformation during exposure to oxidant. Essentially identical responses to oxidation were found in both situations (Table 1), and again, wild-type channels gave no response. These results show that disulfide formation across the T1 subunit interface proceeds readily at both of the channel's conformational extremes: at −80 mV (S4 "in", activation-gate closed, C-type gate open), and at zero voltage (S4 "out", activation-gate open, C-type gate closed).

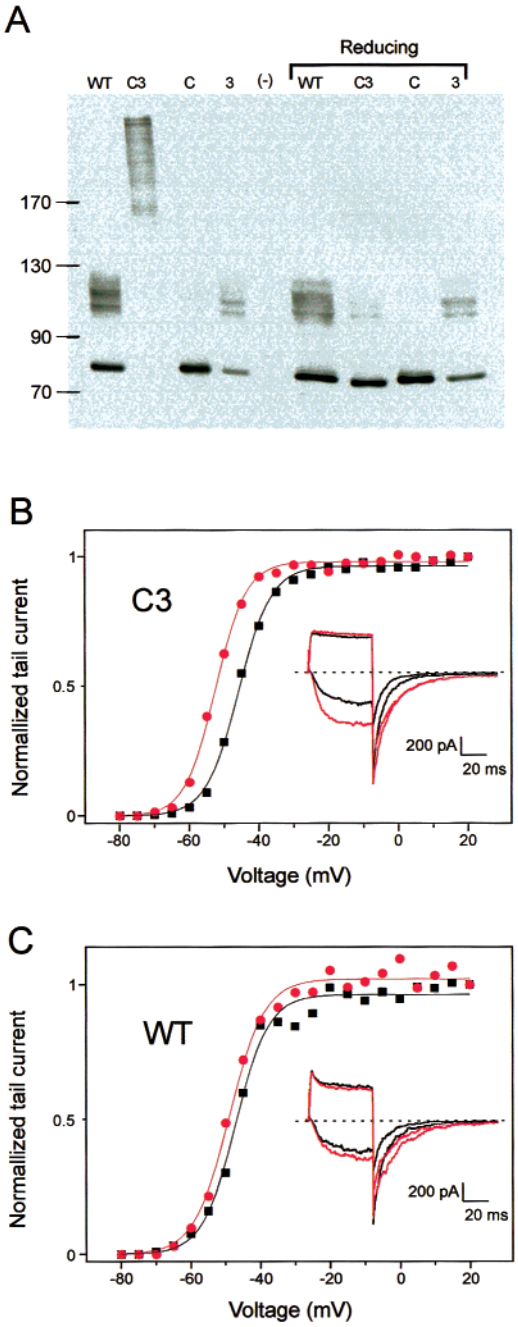

FIGURE 5: Effect of oxidation on voltage-dependent gating. (A) Immunoblot of C3 channels and accompanying controls, as in Figure 4B, except that oxidation was with 0.1% H_2O_2, 2 min. (B) Activation curves for C3 double-mutant channels, before (black) and after (red) H_2O_2 oxidation. Solid curves represent fits to Boltzmann functions, with parameters in Table 1. (Inset) Raw current traces at −45 mV (inward current) and 40 mV (outward current). (C) Activation curves and raw current traces for wild-type channels, as in panel B.

Table 1: Electrophysiological Properties of Double-Cysteine Mutant Channels[a]

	control		H_2O_2		H_2O_2 (pre-inactivated)	
construct	V_o (mV)	z	V_o (mV)	z	V_o (mV)	z
WT	−47 ± 1	5.2 ± 0.2	−48 ± 1	4.9 ± 0.4	−48 ± 2	5.4 ± 1.5
A1	−38 ± 2	7.7 ± 0.6	−49 ± 1	5.8 ± 0.4	−51 ± 2	6.4 ± 1.1
C3	−43 ± 1	5.2 ± 0.3	−49 ± 1	5.0 + 0.3	nd	nd

[a] Parameters reported are means ± SE of 3−10 from individual activation curves, each recorded on a single inside-out macropatch in symmetrical 100 mM K^+. In control conditions, patches were bathed in solutions containing 1 mM DTT to prevent spontaneous oxidation. H_2O_2 exposure conditions were as described in Experimental Procedures, using either standard or pre-inactivation protocols.

DISCUSSION

We have shown that the crystal structure of the isolated T1 domain can be productively used to design disulfide bonds to cross-link Shaker channels across the T1 subunit interface, a predictive success arguing powerfully that the structure exists in the mature, membrane-resident Shaker channel. This conclusion is particularly convincing in light of the failure of mismatched residues to cross-link; since the scrambled pairs cohabit the same interface, this negative control undercuts the often-cogent objection that protein mobility might account for cross-links (*21*). The spectre of protein floppiness is further exorcized by the failure of cross-links to form at three residue-pairs in close proximity, B+2, D+4, and E+5. It is not surprising that some of the cross-subunit residues with closely apposed side chains fail to form cross-links upon cysteine substitution, since the 2 Å S−S bond distance in a typical disulfide is shorter than the 5−6 Å distances between γ-atoms in the natural side chains. Thus, the replacement of a salt bridge by a disulfide bond necessitates subtle adjustments of the polypeptide backbone, which may be tolerated at some positions but forbidden at others. For this reason, we consider the 50% success rate for finding cross-link-competent pairs of close side chains to be remarkably high in a rigid protein structure.

Validation of the T1 domain structure has profound implications for the overall architecture of the Shaker channel. Our results rule out the possibility (*10*) that the isolated domain tetramer exists only as an intermediate in channel assembly and is thereafter altered in conformation. In light of the demonstration (*10*) that the T1 symmetry axis is not part of the ion-permeation pathway, the results imply that the T1 tetramer must be separated from the pore's cytoplasmic entryway rather than continuous with it. In other words, the domain must exist as cartooned in Figure 1C: a cytoplasmic "hanging gondola," suspended by "cables" formed at least in part by the linker sequence between T1 and S1. This, in turn, requires that ions gain access to the cytoplasmic end of the pore laterally through four "windows" bounded by the cables. These windows must be at least 15 Å in diameter, since the N-terminal inactivation peptide readily diffuses from bulk solution to its receptor in the membrane-embedded part of the channel to produce N-type inactivation (*22*−*24*).

Our experiments do not speak to the orientation of T1 on the channel—whether its C-terminus is "up", i.e., pointing toward the membrane, or in the opposite alignment. However, the recent structure of the T1-$K_v\beta$ complex (*8*) argues convincingly that the T1 domain is oriented with the C-terminus toward the membrane, as originally proposed (*3*). The Shaker channel, and by implication all K_v-type channels, must now be viewed as a membrane-embedded structure ~90 Å square and 40 Å thick, with the T1 tetramer, roughly a 35 Å cube, suspended ~20 Å away from the intracellular side of the membrane by connecting links outlining wide access-windows. This inferred picture has been dramatically confirmed by a recent 25-Å resolution three-dimensional struc-

ture of inactivation-removed Shaker determined by electron microscopic image reconstruction (*25*) showing just such a suspended mass, with windows of the expected size. Recently, X-ray and electron crystallography studies have revealed cytoplasmic hanging gondolas in a bacterial mechanosensitive channel (*26*) and a nicotinic acetylcholine receptor (*27*), proteins without known evolutionary relationships to Shaker. From a functional viewpoint, this structural motif is a puzzling curiosity whose biological purpose is still to be understood.

These results directly bear on the current debate regarding the role of the T1 domain in voltage-activation of K^+ channels. On one side of this discourse (*11*, *12*) is the idea that conformational changes in T1 are linked to the voltage-activation gate, with channel opening accompanied by a pulling apart, or "detetramerization" of the domain. This proposal emanates from the identification of point mutations that stabilize the open channel, as seen by leftward voltage-activation shifts, and concomitantly destabilize the water-soluble domain, as measured through urea-denaturation profiles. On the other side (*10*) is the observation that complete removal of T1 from Shaker produces only minor perturbation in the relative free energy of open vs closed conformations. In general, we consider the leftward and rightward activation gating-shifts observed by all contenders in this debate to be so small (equivalent to 1 kcal/mol or less) as to be mechanistically uninformative, falling in the range of gating-shifts arising from altered ionic conditions, directed mutations, or modulatory fine-tuning throughout K^+ channel sequences (*28*−*33*), including some in the T1 region (*34*). We are unpersuaded by the correlation of denaturation characteristics and gating shifts, since this was based on only two mutants, while a third that contradicted the correlation was excluded from the analysis (*12*). Our demonstration that disulfide cross-links across the T1 subunit-interface promote, rather than hinder, channel opening rebuts the argument that the domain must spread apart for the channel to open. This open-state stabilization occurs upon cross-linking at either of two different locations in the interface—A1, near the top of the domain and C3, buried deeply within it—and thereby places constraints on any structural models of the putative linkage of T1 movements to voltage-dependent gating.

ACKNOWLEDGMENT

We are grateful to Drs. Niko Grigorieff and Rod MacKinnon for sharing their results with us prior to publication and Rob Blaustein for dispassionate criticisms on the manuscript.

REFERENCES

1. Sigworth, F. J. (1994) *Q. Rev. Biophys. 27*, 1−40.
2. Yellen, G. (1998) *Q. Rev. Biophys. 31*, 239−295.
3. Kreusch, A., Pfaffinger, P. J., Stevens, C. F., and Choe, S. (1998) *Nature (London) 392*, 945−948.
4. Bixby, K. A., Nanao, M. H., Shen, N. V., Kreusch, A., Bellamy, H., Pfaffinger, P. J., and Choe, S. (1999) *Nat. Struct. Biol. 6*, 38−43.
5. Li, M., Jan, Y. N., and Jan, L. Y. (1992) *Science 257*, 1225−1230.
6. Shen, N. V., and Pfaffinger, P. J. (1995) *Neuron 14*, 625−633.
7. Sewing, S., Roeper, J., and Pongs, O. (1996) *Neuron 16*, 455−463.
8. Gulbis, J. M., Zhou, M., Mann, S., and MacKinnon, R. (2000) *Science 289*, 123−127.
9. Pfaffinger, P. J., and DeRubeis, D. (1995) *J. Biol. Chem. 270*, 28595−28600.
10. Kobertz, W. R., and Miller, C. (1999) *Nat. Struct. Biol. 6*, 1122−1125.
11. Choe, S., Kreusch, A., and Pfaffinger, P. J. (1999) *Trends Biochem Sci. 24*, 345−329.
12. Cushman, S. J., Nanao, M. H., Jahng, A. W., DeRubeis, D., Choe, S., and Pfaffinger, P. J. (2000) *Nat. Struct. Biol. 7*, 403−407.
13. Molday, R. S., and MacKenzie, D. (1983) *Biochemistry 22*, 653−660.
14. Oprian, D. D., Molday, R. S., Kaufman, R. J., and Khorana, H. G. (1987) *Proc. Natl. Acad. Sci. U.S.A. 84*, 8874−8878.
15. Schulteis, C. T., Nagaya, N., and Papazian, D. M. (1996) *Biochemistry 35*, 12133−12140.
16. Sun, T., Naini, A. A., and Miller, C. (1994) *Biochemistry 33*, 9992−9999.
17. Rudy, B., and Iverson, L. E. (1992) *Methods Enzymol. 207*, 225−345.
18. Laemmli, U.K. (1970) *Nature (London) 227*, 680−685.
19. Liman, E. R., Tytgat, J., and Hess, P. (1992) *Neuron 9*, 861−871.
20. Santacruz-Toloza, L., Huang, Y., John, S. A., and Papazian, D. M. (1994) *Biochemistry 33*, 5607−5613.
21. Careaga, C. L., Sutherland, J., Sabeti, J., and Falke, J. J. (1995) *Biochemistry 34*, 3048−3055.
22. Zagotta, W. N., Hoshi, T., and Aldrich, R. W. (1990) *Science 250*, 568−571.
23. Isacoff, E. Y., Jan, Y. N., and Jan, L. Y. (1991) *Nature (London) 353*, 86−90.
24. Holmgren, M., Jurman, M. E., and Yellen, G. (1996) *J. Gen. Physiol. 108*, 195−206.
25. Sokolova, O., Kolmakova-Partensky, L., and Grigorieff, N. (2000) (manuscript in preparation).
26. Chang, G., Spencer, R. H., Lee, A. T., Barclay, M. T., and Rees, D. C. (1998) *Science 282*, 2220−2226.
27. Miyazawa, A., Fujiyoshi, Y., Stowell, M., and Unwin, N. (1999) *J. Mol. Biol. 288*, 765−786.
28. Swenson, R. P., and Armstrong, C. M. (1981) *Nature (London) 291*, 427−429.
29. Monks, S. A., Needleman, D. J., and Miller, C. (1999) *J. Gen. Physiol. 113*, 415−423.
30. Li-Smerin, Y., Hackos, D. H., and Swartz, K. J. (2000) *J. Gen. Physiol. 115*, 33−50.
31. Gonzalez, C., Rosenman, E., Bezanilla, F., Alvarez, O., and LaTorre, R. (2000) *J. Gen. Physiol. 115*, 193−208.
32. Peretz, A., Sobko, A., and Attali, B. (1999) *J. Physiol. (London) 519*, 373−384.
33. Wang, Q. (1999) *Ann. N. Y. Acad. Sci. 868*, 447−449.
34. Huang, X. Y., Morielli, A. D., and Peralta, E. G. (1994) *Proc. Natl. Acad. Sci. U.S.A. 91*, 624−628.

BI001292J